ROYAL SOCIETY
OF CHEMISTRY

Predictive modelling and optimization of lignin extraction efficiency and quality in birch-wood mild ethanosolv fractionation in a semi-continuous flow-through reactor

Amponsah Preko Appiah, [ID] Bertran-Llorens Salvador, [ID]
Pelle van Aefst [ID] and Peter J. Deuss [ID] *

Lignin, a complex and abundant biopolymer found in plants, holds immense potential for sustainable materials and chemicals. However, conventional extraction methods often lead to structural deterioration of the native-like aryl ether structure *via* condensation and other chemical alterations, limiting lignin utility. High delignification in conjunction with preservation of the versatility and functionality of lignin structure for high-value applications can be achieved using advanced mild extraction techniques. In this study, an integrated modeling–experimental approach is used to attain a scalable framework for lignin-first biorefining. Temperature and flow rate were optimized in a flow-through mild ethanosolv system utilizing crude birch-wood chips (without extractive-removal) to balance solvent use, delignification, and structure preservation. Delignification and lignin yield were monitored separately as was its quality in terms of preservation of its native aryl-ether structure, as determined *via* 2D HSQC NMR and GPC. Extraction kinetics were monitored using UV-Vis spectroscopy to allow for maximizing efficient solvent utilization. Response surface methodology identified optimal conditions (145–151 °C, 8 $g_{solvent}$ min^{-1} flow rate), revealing temperature as the primary driver for extraction, exhibiting synergistic effects with the flow rate. Notably, higher flow rates at elevated temperatures ($\geq$140 °C) mitigated β-O-4 linkage degradation without compromising delignification efficiency. Experimental validation of the optimized model at 150 °C and 8 $g_{solvent}$ min^{-1} achieved 82 wt% delignification and yielded lignin with high β-O-4 linkage content (59.4 per 100 aromatic units (ArU)), aligning closely with model predictions (81–87 wt%, $\geq$52 β-O-4 per 100 ArU). Solvent consumption was optimized from the model (13.1 mL g^{-1}, solvent : biomass) and realized a reduction of over 40% of solvent consumption when compared with solvent consumption from typical batch organosolv systems (22.9 mL g^{-1}, solvent : biomass). Finally, the optimization reduced the extraction time significantly from typically 2 hours to 30 min

University of Groningen, Faculty of Science and Engineering, Department of Chemical Engineering, Engineering and Technology Institute of Groningen, Netherlands. E-mail: p.j.deuss@rug.nl; a.p.appiah@rug.nl; s.bertran. llorens@rug.nl; p.van.aefst@student.rug.nl

when compared with previous standard extraction conditions (120 °C, 2 $g_{solvent}$ min^{-1} flow rate), without compromising on extraction efficiency and lignin quality. This study shows the potential of mild organosolv extraction with alcohol with optimized conditions.

1 Introduction

Birch wood (genus *Betula*) is a predominant hardwood native to temperate and boreal regions, particularly abundant in Northern Europe and Canada. Despite its widespread availability and advantageous chemical composition, birch wood remains underutilized in industrial processing[1,2] due to challenges associated with its high hemicellulose content and structurally complex lignin, which can hinder conventional pulping and downstream operations. Consequently, substantial volumes of birch wood are used for low-value energy production, or discarded as waste.[1,3] As sustainable, non-food lignocellulosic feedstocks gain prominence, birch wood has emerged as a prominent substrate for biomass valorization and in particular in research related to lignin extraction and utilization.

Lignin as a heterogenous polymer comprises mainly of three phenylpropanoid monomers: *p*-coumaryl alcohol, coniferyl alcohol, and sinapyl alcohol. These monolignols form the building blocks of lignin, polymerizing into *p*-hydroxyphenyl (H), guaiacyl (G), and syringyl (S) units, respectively (Fig. 1). The relative abundance of these units depends, among other environmental factors, on the plant species, and birch as a hardwood consists mostly of S and G units.[4] Lignin's complex structure is characterized by various types of linkages between these units, with the aryl ether β-O-4 linking motif being the most common, accounting for 50–66% of all linkages in native-like birch-wood lignin.[5] Other important linkages include 4-O-5, β-5, and β-β.[4,6] (Fig. 1).

Lignin accounts for up to 30% of lignocellulosic biomass and plays a critical role in developing sustainable biorefining strategies.[7,8] Historically, conventional biorefineries have prioritized carbohydrate valorization using processes that induce degradation of the lignin aryl ether structure and subsequent C–C bond formation *via* condensation, increasing lignin recalcitrance and making it more
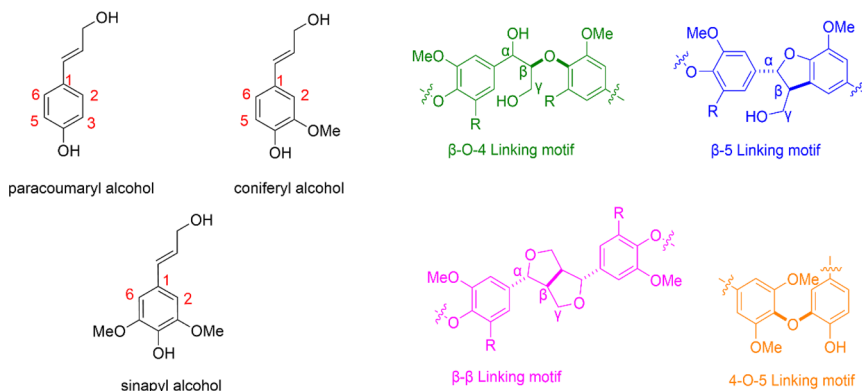

Fig. 1 Chemical structure of the three phenylpropanoid monomers of lignin and major lignin linking motifs highlighting the inter-unit bonds.

difficult to obtain added-value products such as aromatic monomers.[8,9] The conservation of the native structure of the lignin, mainly the β-O-4 linkages, as the dominant C–O bonds, is essential for controlled depolymerization into valuable monomers and for post-modifications for high-end applications as a oligomer/polymer.[10,11] For example, the selective cleavage of β-O-4 linkages through mild catalytic conditions has resulted in high yields of aromatic monomers, which can serve as the starting point for the synthesis of fine chemicals that could lead to a number of polymer building blocks.[12] Shuai *et al.*[13] also demonstrated that protecting β-O-4 linkages with formaldehyde stabilization during lignin delignification is important for obtaining high yields of aromatic monomers *via* the catalytic depolymerization pathway, emphasizing the importance of β-O-4 retention in lignin valorization and concluding that subsequent valorization into monomers only succeeds when β-O-4 linkages are retained during pretreatment. In another study, Deuss *et al.*[14] demonstrated a strong correlation between the yield of phenolic acetals from Fe(OTf)$_3$-catalyzed lignin depolymerization, and the β-O-4 content of the lignin feedstock, where lignins with higher abundance of β-O-4 produced much higher monomer yields, clearly indicating once again that preservation of β-O-4 linkages is an important requirement for effective downstream valorization.

This "lignin-first" approach emphasizes lignin valorization by integrating lignin stabilization during extraction. This paradigm shift enables access to a broader array of high-value aromatic compounds, challenging lignin's traditional role as a low-value fuel source.[9,15,16] There are several lignin-first methods such as reductive catalytic fractionation (RCF) and oxidative catalytic fractionation (OCF), used to obtain monomers,[16,17,19] as well as aldehyde or alcohol protection methods that have proven to be successful at protecting the lignin structure from condensation, thus allowing the efficient isolation of high-aryl-ether-content lignin (*e.g.*, >50 per 100 aromatic units (ArU)).[18]

Traditional batch organosolv systems suffer from prolonged lignin exposure to reactive conditions, promoting degradation, condensation, and redeposition onto solids. The reported lignin yields and quality from some batch processes range between 2 to 11 wt% and 12 to 25 per 100 ArU, respectively.[14,20,21] To overcome such limitations, semi-continuous flow-through organosolv systems have been developed. These systems reduce the residence time of extracted reactive lignin fragments and improve mass transfer, enhancing both delignification efficiency and β-O-4 preservation.[4,15,22–24] Zijlstra *et al.*[23] reported an efficient flow-through butanosolv system at mild temperatures (120 °C) using different biomasses.[23] These conditions were also applied for ethanol, which showed yields of 74% delignification and a high lignin quality of 59 β-O-4 per 100 ArU that could be even further increased with a supercritical-CO$_2$ pretreatment.[22,24,25] The mild conditions used by the authors achieve a high β-O-4 retention compared to other flow-through extractions with harsher conditions, such as the work of Kramarenko *et al.*,[26] who used a 1 : 1 methanol–water mixture at 140–200 °C, achieving 88 wt% delignification but a β-O-4 content of 19 per 100 ArU, indicating the trade-off between efficiency and structural preservation at high temperatures.

These advances underscore the potential of flow-through organosolv systems for recovering high-quality lignin suitable for high-value applications, particularly when process conditions are carefully optimized to balance delignification and structural integrity. Therefore, further optimization is needed to enhance native-

like lignin extraction, reduce solvent consumption, and address scalability for industrial applications.

This study presents a methodical investigation into the optimization of a modified flow-through ethanosolv system for lignin extraction from birch wood. The research focuses on two critical process variables: temperature and solvent flow rate. UV-Vis spectrophotometry was used to provide insight into the lignin extraction kinetics in the flow-through system. Response surface methodology (RSM) was employed to evaluate the impact of the selected parameters on the key aspects of the extraction process: delignification efficiency, lignin structural integrity and quality, and the extent of alcohol incorporation into the lignin structure. By employing this approach, we aim to explore the complex interplay between process conditions and extraction outcomes in terms of delignification efficiency and extracted lignin quality. At the same time solvent use is optimized as this is one of the key factors, alongside solvent recycling efficiency, that impact the economic potential of large-scale lignin processing.[27,28]

2 Materials and methods

2.1 Solvents, chemicals and biomass

The solvents and chemicals used for this research work were sourced as follows:

Absolute ethanol was purchased from J. T. Baker – Avantor Performance Materials Poland S. A., acetone from Macron Fine Chemicals – Avantor Performance Materials Poland S. A., sulfuric acid (95–97 wt%) from Merck KGaA – Darmstadt Germany, sulfuric acid (72 wt%) from Chem-lab NV – Belgium, and sodium hydroxide, acetone d_6 99.9 atom % D and deuterium oxide 99.9 atom % D all from Sigma-Aldrich.

Birch wood (*Betula pubescens*) was locally sourced and used as the biomass for this research. Refer to Table S1 in the SI section for detailed compositional analysis of the birch-wood biomass.

2.2 Flow-through reactor configuration and operation

Birch-wood feedstock was debarked and shredded by means of a low-speed granulator to a particle size of 0.56–1.00 mm. The biomass was not processed for extractive removal, as initial studies indicated the possibility of successfully extracting lignin from unprocessed birch-wood biomass with high efficiency. Samples were stored in airtight zip-lock bags to prevent moisture fluctuation prior to experimentation.

Flow-through extraction was carried out using a custom-built reactor system designed to maintain precise control over solvent delivery, temperature, and extract collection, enabling reproducible results under standardized conditions. The extraction was done as previously reported.[22–25] In a typical extraction procedure, approximately 20 g of biomass were loaded in the reactor column. The solvent (4 : 1 ethanol–water mixture with 0.18 M H_2SO_4.) was pumped through the heated reactor at a controlled flow rate specific to the experimental conditions of the run being conducted. Extractions were not limited by time but by the amount of solvent pumped through the reactor. A solvent-to-biomass ratio of 18 $mL_{solvent}$ $g_{biomass}^{-1}$ was chosen. Therefore, even though the flow rate varied in different runs, the solid-to-liquid ratio was maintained. Per the solvent biomass ratio,

360 mL of solvent was required for each extraction. However, a little in the excess of 400 mL of solvent was used to compensate for the reactor dead volume. An automated sample collector retrieved aliquots of the extract at predetermined intervals, enabling time-resolved analysis of extraction kinetics.

Lignin extraction was monitored using ultraviolet-visible (UV-Vis) spectroscopy. The molar absorptivity coefficient (ε) of birch lignin was determined using a representative lignin sample (refer to SI 1.1 for lignin extraction specifics), corrected *via* 2D-HSQC NMR for carbohydrate content, to estimate purity.[23] These purity-corrected values refined the calibration curve (refer to SI Fig. S2), improving quantification accuracy.

Following the extraction, lignin was precipitated using a previously established method from the literature.[25,29] In brief, the liquors collected over time for each run were combined and adjusted to a pH of 5–6 using sodium hydroxide, concentrated *via* rotary evaporation, and redissolved in 30 mL of acetone (99.5%). This solution was added dropwise to 300 mL of acidified water (pH 1, adjusted with sulfuric acid) under vigorous stirring. Lignin precipitated from solution was allowed to settle before isolation by vacuum filtration. The solid lignin was finally dried overnight in a vacuum oven at 35 °C. A schematic overview of the entire process is shown in Fig. 2. (See SI Fig. S1. for the Piping & Instrumentation Diagram of the flow-through reactor).

2.3 Biomass composition analysis (structural carbohydrates & lignin)

The lignocellulosic composition of birch-wood biomass was quantitatively evaluated for both the untreated feedstock and the delignified pulp across all experimental runs to assess delignification efficiency and structural modifications. A comprehensive compositional analysis was conducted, including acid-insoluble lignin, acid-soluble lignin, and structural carbohydrates (glucan, xylan, and arabinan) to characterize cellulose and hemicellulose fractions. Quantification followed the NREL/TP-510–42618 protocol,[30] employing a two-step acid hydrolysis: initial treatment with 72% sulfuric acid, followed by dilution to 4% for secondary hydrolysis. Monosaccharides were quantified *via* HPLC using an Agilent 1200 pump equipped with a Bio-Rad organic acid column (Aminex HPX-87H), a refractive index detector, and a UV detector (210 nm). The HPLC column was operated at 60 °C, and a 5 mM aqueous sulfuric acid solution was used as the
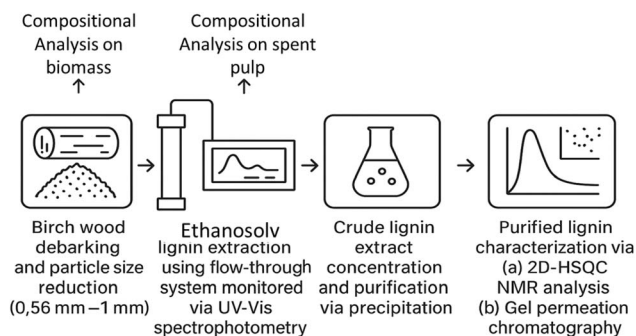

Fig. 2 Flow diagram of the experimental processes (generated with Sora AI).

mobile phase with a flow rate of 0.55 mL min^{-1}. The injection volume was set at 5 μL. The concentrations of individual compounds in the product mixture were determined using calibration curves obtained by analyzing standard solutions of known concentrations. The Acid Soluble Lignin (ASL) was measured *via* UV with a quartz cuvette in an Agilent CrossLab Cary 60 UV-Vis spectrophotometer. Acid-insoluble lignin was measured as the weight difference in the filter crucible after drying the sample at 105 °C and corrected for the ash obtained after calcination at 575 °C. Moisture was measured with a PCE-MA 110 moisture meter.

2.4 NMR analysis

2D-HSQC NMR spectroscopy was used for lignin structural analysis and recorded on a 600 MHz Bruker Biospin (BASIC PROBHD, Rheinstetten, Germany) instrument. A 60 mg lignin sample was dissolved in 0.6 mL of acetone-d_6 with a few drops of deuterium oxide to ensure complete dissolution. Spectra were acquired with acetone-d_6 as the internal reference (δ_C 29.84, δ_H 2.05 ppm). The Bruker pulse sequence 'hsqcetgpsisp.2' was applied for the ^{13}C–^{1}H correlation experiment. Data acquisition used 1024 points (11–0 ppm) in F2 (^{1}H, 131 ms) and 512 increments (160–0 ppm) in F1 (^{13}C, 6 ms), with 4 scans and a 1.5 s delay, totaling 1 hour. Data were analyzed using MestReNova 14; the integration region and calculations were done according to previous works.[24]

2.5 GPC analysis

For gel permeation chromatography (GPC) analysis, 10 mg of dried lignin was dissolved in 1 mL of tetrahydrofuran (THF) with a drop of toluene as an internal standard. The solution was filtered through a 0.45 μm syringe and analyzed using a Hewlett Packard 1100 series with a 20 μL injection volume and THF as the mobile phase. The calibration standards were polystyrene with a calibrated range of 200–10 000 Da. The software then calculated the molecular-mass distribution of the lignin sample.

2.6 Experimental design (DOE)

A response surface methodology (RSM) design of experiment was made incorporating two factors, each examined at three levels, while measuring three distinct responses. The factors, levels, and responses are detailed in Tables 1 and 2.

The final experimental design and runs were generated with Design Expert from StatEase software and are detailed in Table 3.

The time intervals for the extract sampling (Table 3) were adjusted based on the flow rate of each experiment in order to accommodate the maximum capacity of the sampling vials (20 mL). For monitoring of the lignin extraction over time,

Table 1 Factors and levels used in the design of experiment

Factors	Level 1	Level 2	Level 3
Temperature (degrees C)	120	140	160
Flow rate ($g_{solvent}$ min^{-1})	2	4	8

Table 2 Responses and their measurement for the design of experiment

Responses	As determined by
Lignin quality (aryl-ether bonds)	Number of β-O-4 linkages per 100 aromatic units
% alcohol incorporation	The degree of α-alkoxylation
% delignification	Amount of lignin extracted from biomass

the volumes collected in each vial were accounted for and factored into all calculations.

3   Results & discussion

3.1   Lignin extraction efficiency

Lignin extraction efficiency (delignification) under different flow rates and temperatures (as per Table 3) was assessed by comparing the lignin content in the biomass prior to the extraction with the lignin content in the pulp after extraction (Fig. 3). At the same time, insight into the extraction kinetics was obtained by following the UV-absorbance of the effluent at set intervals (Fig. 4). The efficiency of lignin extraction observed in this study reveals a consistent and interconnected relationship among the delignification results, UV-Vis monitored extraction profiles, and the actual recovered lignin yields, apart from specific data points discussed below (Fig. 5). However, note that absolute lignin UV-Vis extraction profiles cannot be directly compared due to changes to the extinction coefficient for lignin extracted under different conditions (*vide infra*).

Lignin extraction for all the runs were ended when approximately 360 mL of solvent (in accordance with the solvent : biomass ratio of 18 $mL_{solvent}$ $g_{biomass}{}^{-1}$) were used. Extraction times varied inversely with respect to flow rates (Table 4). For example, when the flow rate was increased from 2 g min^{-1} to 8 g min^{-1}, there was a proportional reduction in total extraction time from 150 minutes to 38 minutes. A higher volumetric flow also results in decreased contact time between biomass and the solvent and shorter residence time for extracted compounds including lignin.

Delignification improved significantly with temperature, increasing from 57.6–74.1 wt% at 120 °C to 80–89 wt% at 140 °C and reaching 93.5–94.9 wt% at 160 °C (Fig. 3). These values exceed most of the reported values in the literature

Table 3 DOE with experimental runs

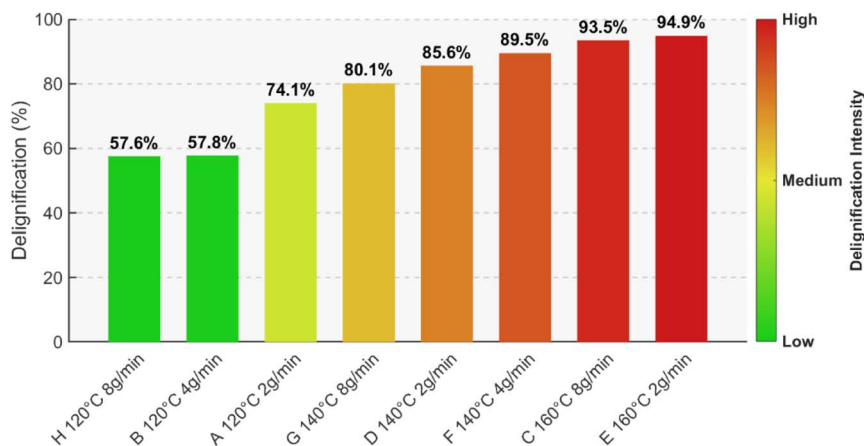| Runs	Temperature (°C)	Flow rate ($g_{solvent}$ min^{-1})	Extract sampling interval (mins)
A	120	2	5
B	120	4	3
C	160	8	2
D	140	2	5
E	160	2	5
F	140	4	3
G	140	8	2
H	120	8	2

Faraday Discussions

Fig. 3 Delignification based on the compositional analysis on the crude biomass and the pulp obtained after lignin extraction (see SI Table S2 for details on quantified lignins based on the mass balance).
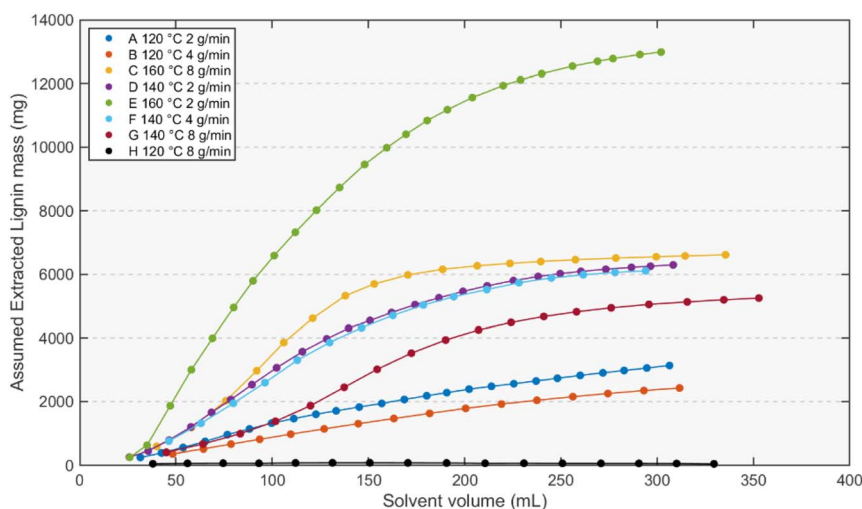

Fig. 4 Plot of accumulated lignin mass *vs.* solvent use from the UV-Vis spectrophoto-metric monitoring of the flow-through extraction kinetics calibrated using an extinction coefficient obtained from a reference isolated birch lignin.

(76.0–76.3 wt%),[22,31] equalling the 93–98% previously reported for butanosolv extraction.[23] Flow-rate effects were temperature-dependent: at 120 °C, a lower flow (2 $g_{solvent}$ min^{-1}, run A) outperformed higher-flow runs (B and H), indicating longer-residence-time benefits under mild conditions. However, at 160 °C, both low (run E) and high (run C) flow rates achieved high delignification, highlighting temperature as the dominant driver. While previous studies[22,23] reported positive effects of increased flow during biomass pretreatment, this study shows that flow rate is more impactful at lower temperatures, where residence time governs the main reactivity.
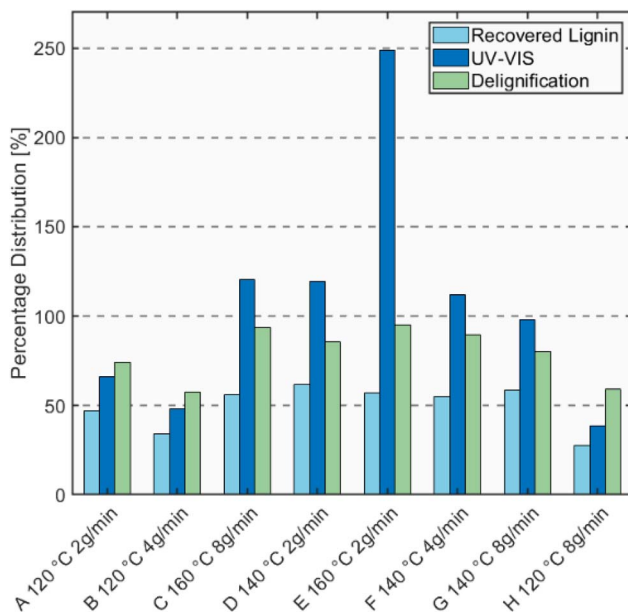
Fig. 5 Comparison of lignin extraction obtained from different processing conditions including: lignin recovery from the purification process (recovered lignin), lignin yield from calibrated UV-Vis and lignin yield calculated based on the lignin content in the extraction residue (delignification).

Table 4 Flow rates and their corresponding extraction times per minute as well as the total extraction times for the selected flow rates in the experimental runs

Flow rate (g min^{-1})	Volume/min (mL min^{-1})	Total extraction time (mins)
2	2.4	150
4	4.7	77
6	7.1	51
8	9.4	38

UV-Vis monitoring (Fig. 4) further supports these findings: higher temperatures led to steeper extraction curves and faster lignin solubilization. However, most runs showed a plateau phase, *e.g.*, run C extracted 6.6 mg of lignin with 335 mL of solvent, indicating saturation of extractable lignin and that the solvent use can be optimized to the conditions *via* UV-Vis monitoring (*vide infra*). Lower-temperature runs (A, B and H at 120 °C) showed slower extraction kinetics and lower yields, especially at higher flow (run H), where limited residence time hindered sufficient contact time and mass transfer. The positive effect of the increased flow rate on mass transfer has been shown before for lignin extraction using different solvent systems and operating conditions.[32,33] These findings highlight a synergistic interaction between temperature and flow rate.

Despite the general agreement between UV-Vis trends, delignification data and isolated lignin, significant overestimations by UV-Vis quantification were

observed under certain conditions by using calibration with a single isolated lignin (see Fig. 5). Most notably, in run E, the UV-Vis estimated lignin yield reached 249% (12.2 g), far exceeding the theoretical maximum of 4.9 g lignin for the biomass used. This overestimation is attributed to the formation of degradation products, which interfere with absorbance measurements at 279 nm, a known limitation of UV-Vis spectroscopy.[34] Lignin extracted at 120 °C was used for calibration and does not reflect structural changes to the lignin obtained at higher temperatures. Thus, although useful for real-time monitoring, UV-Vis lacks the capacity to distinguish lignin extracted under different conditions. While developing temperature-specific calibration curves (e.g., for 120 °C, 140 °C and 160 °C) would improve accuracy, this was not pursued here, as UV-Vis was used solely for process monitoring. The amount of recovered lignin adjusted for the level of alcohol modification (as determined via 2D HSQC NMR, see below) and moisture content followed the general trend of delignification, albeit lower. This is explained by the incomplete precipitation of lignin from the solvent or by an ineffective filtration step, which have been addressed in different works.[35]

Collectively, the analysis of delignification kinetics via UV-Vis monitoring and the delignification efficiency obtained from lignin quantification in the recovered biomass demonstrate that temperature is the dominant factor influencing lignin extraction efficiency, while flow rate shows a temperature-dependent behavior, enhancing extraction at lower temperatures through prolonged residence time, but playing a less important role under higher temperature conditions.

3.2 Lignin quality analysis

Assessing the quality of the extracted lignin in terms of chemical structure retention is just as crucial as evaluating the delignification efficiency when determining the effectiveness of the flow-through extraction method. The molecular architecture and compositional heterogeneity of lignin are profoundly influenced by extraction conditions such as temperature and solvent flow rate.[4,15,22,23] To assess the chemical structure, GPC (SI Table S3) and 2D HSQC NMR (Fig. 6 and 7) analysis were performed.

GPC results show number-average molecular weights (M_n) between 1064 and 1484 g mol^{-1}, well within the range reported for lignins obtained via organosolv or flow-through extraction methods.[36] However, the weight-average molecular weight (M_w) range of 2500 to 3900 g mol^{-1} observed with the extracted lignin is on the high side of the literature-reported range of M_w, typically 500–5000 g mol^{-1}.[36] This observation is in agreement with observed trends with alcohol extractions of lignin resulting in structural modifications of lignins with alcohol groups, which allow for the extraction of high-molecular-weight fragments due to increased solubility.[29]

The typical 2D HSQC NMR spectrum (Fig. 6) shown for run B (120 °C, 4 g$_{solvent}$ min^{-1}) confirms that the isolated lignin is primarily composed of syringyl (S) and guaiacyl (G) units, with no detectable p-hydroxyphenyl (H) units. A high retention of β-O-4 content is achieved, which is in line with earlier mild organosolv alcohol extractions reported in the literature.[22,24,29] The semi-quantification shows that this is the case for most runs with a β-O-4 content ranging between 50-63 per 100 ArU for these samples (Fig. 7) consistent with the hardwood origin of birch wood.[37] (See SI Fig. S3–S11 for NMR spectra of all runs).
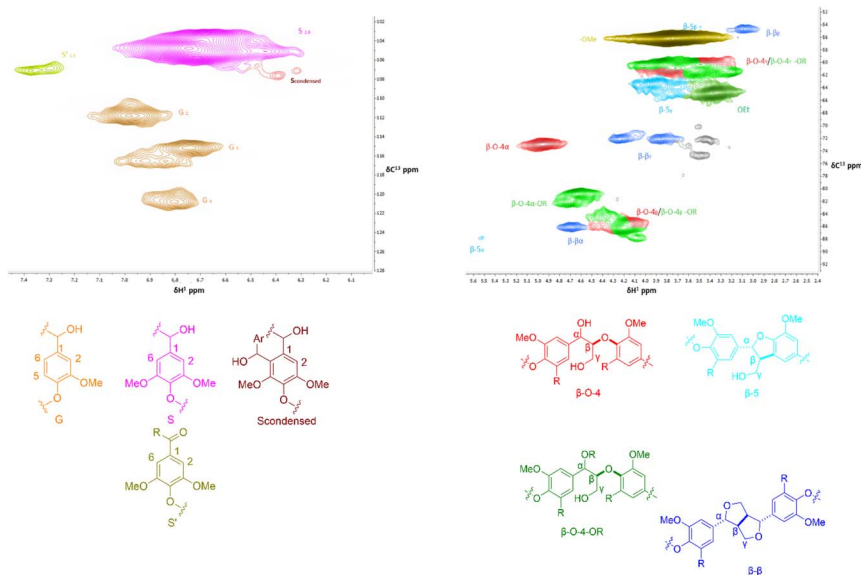
Fig. 6 2D-HSQC NMR of organosolv-extracted birch-wood lignin showing the lignin aromatic subunit region (left) and linking motif region (right) for run B (120 °C, 4 g$_{solvent}$ min^{-1}), done in acetone d_6.
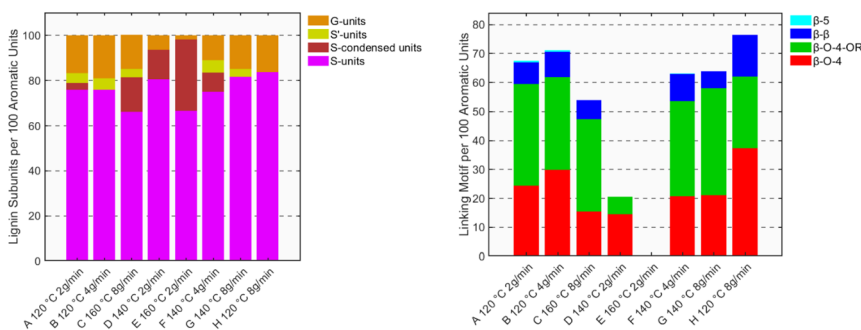

Fig. 7 Distribution of lignin linking motifs (left) and lignin subunits (right) quantified from 2D-HSQC NMR semi-quantification for the runs (A to H). Data can be found in SI Table S4.

The samples extracted at low temperatures (120 °C, runs A, B and H) display greater preservation of β-O-4 linkages and less evidence of structural condensation (higher aryl ether linkage content in the linkage region and lower S$_{cond}$ (Syringyl condensed units) in the aromatic region). Run A and run B, with flow rates of 2 and 4 g$_{solvent}$ min^{-1} respectively, maintain β-O-4 contents above 59 per 100 ArU, with relatively high M_w values (3612 and 3766 g mol^{-1}). This suggests relatively low lignin bond cleavage and minimal condensation. These runs also exhibited balanced S/G ratios (4.2–5.1) with a general trend that higher extraction efficiency and higher β-O-4 contents are concurrent with higher S unit content as observed before.[22]

Run H (120 °C, 8 g$_{solvent}$ min^{-1}), demonstrates the highest β-O-4 content (62.0 per 100ArU) and a complete absence of S$_{cond}$ units, indicating that both low

thermal severity and high flow rate jointly support the extraction of structurally intact lignin, but, as shown in the previous section, with a lower yield of 58 wt%.

At 140 °C, lignin structure is highly affected despite the modest temperature increase. Run D (2 $g_{solvent}$ min^{-1}) shows the lowest β-O-4 content among samples with quantifiable linkages (20.5 per 100 ArU), a relatively high level of S_{cond} units (8.2%), all indicating the formation of condensation products. In contrast, runs F and G, carried out at the same temperature but with increased flow rates (4 $g_{solvent}$ min^{-1} and 8 $g_{solvent}$ min^{-1}, respectively), exhibit markedly improved structural preservation. β-O-4 linkages increase to 53.6 per 100 ArU in run F and 58.0 per 100 ArU in run G, while condensation is notably reduced. These changes suggest that higher flow rates effectively mitigate lignin degradation at this temperature by facilitating faster removal of solubilized fragments. GPC profiles further support this trend: run F shows the lowest M_n and M_w, (1064 and 2518 g mol^{-1}) indicating smaller fragments, whereas run D has a higher M_n and M_w (1334 and 3563 g mol^{-1}), likely due to some condensation of fragments in line with the higher S_{cond}.

A similar, yet more pronounced, pattern is observed at 160 °C, as seen in runs C and E. Despite identical extraction temperatures, these runs yield markedly different results due to their flow rates. Run C (8 $g_{solvent}$ min^{-1}) retains a substantial amount of β-O-4 linkages (47.2 per 100 ArU), suggesting limited structural breakdown. In contrast, run E (2 $g_{solvent}$ min^{-1}) shows a complete loss of β-O-4 linkages, and the highest content of S_{cond} units (23.6%), all pointing to extensive depolymerization and condensation. These results are consistent with literature reports by Crestini et al.[36] and Zijlstra et al.,[22] which highlight that high temperature promotes β-O-4 cleavage and the formation of C–C linkages through electrophilic aromatic substitution. However, such degradation can be significantly reduced using increased flow. As also demonstrated by Rinaldi et al.,[38] increased flow rates shorten the residence time, suppressing recondensation and preserving structurally relevant features. Thus, while temperature clearly drives reactivity, the contrasting outcomes between runs C and E underscore the critical role of flow rate and residence time in determining lignin structural integrity.

Together with the delignification and lignin yield discussed above, these results emphasize that while temperature is a primary driver for efficient lignin extraction, the flow rate, and by extension, residence time, is a critical process variable for modulating the extent of lignin chemical structural preservation.

3.3 Influence of extraction conditions on lignin alkoxylation

As observed in Fig. 6, alkoxylation occurs simultaneously with lignin extraction *via* incorporation of ethanol in the β-O-4 motif (forming β-O-4-OR). This process can have significant implications for lignin valorization. Enhanced alcohol incorporation has been directly correlated with improved solubility in polar media and influencing catalytic depolymerization efficiency.[29,39] Furthermore, the stabilization of α-carbon positions through etherification has been shown to prevent undesirable repolymerization during downstream processing.[40] These structure–property relationships underscore the importance of precise control over extraction conditions to tailor lignin functionality for specific applications.

The degree of alcohol incorporation into lignin's β-O-4 linkages was found to be significantly influenced by the extraction parameters, as revealed by

quantitative NMR analysis (see SI Tables S4 and S5). Moderate alkoxylation was observed at 120 °C (39.9–59.0% β-O-4-OR of the total β-O-4) with increased flow-rate leading to lower alkoxylation. Significantly higher alkoxylation (>60%) was consistently achieved under intermediate temperature conditions (140 °C) when combined with moderate to high flow rates (4–8 $g_{solvent}$ min^{-1}), as demonstrated by runs F (61.4%) and G (63.3%). These conditions appeared to facilitate effective reagent penetration while maintaining structural integrity of the β-O-4 linkages.

At elevated temperatures (160 °C), run C (8 $g_{solvent}$ min^{-1}) exhibited the highest alcohol incorporation (67.7%), likely due to the increased stability of this motif over the unmodified motif. These results suggest that the level of alkoxylation can be tuned through a careful balance of temperature and flow parameters.

3.4 Optimization study

As observed in the extraction runs, the relationship between flow rate and temperature and how these influence yield and lignin quality is not linear but rather dependent on the synergetic interactions of the aforementioned parameters. Moreover, a trade-off becomes evident between achieving high delignification yields and preserving lignin structure. To better understand these dynamics and identify the optimal operating conditions that balance yield and structural integrity, a predictive model was developed.

Experimental data assessing delignification efficiency, lignin structural integrity, and alcohol incorporation were compiled and analyzed using response surface methodology (RSM). This statistical approach enabled both process-parameter optimization for the flow-through system and mechanistic understanding of parameter–response relationships. Through Design Expert software, three-dimensional response surface models were generated to visualize experimental trends and identify optimal extraction conditions. These models facilitate the design of a precisely controlled system capable of producing tailored lignin products. The resulting predictive models are presented in Fig. 8. Statistical evaluation of the models is presented in Table 5 below.

The delignification model (A) characterizes the effect of extraction temperature and solvent flow rate on the efficiency of lignin removal from birch-wood biomass. The 3D surface illustrates a strong positive correlation between temperature and delignification, with increased values leading to higher lignin solubilization. Likewise, higher solvent flow rates also contribute positively, although with a less pronounced gradient, suggesting a secondary role compared to temperature.

The relatively planar nature of the surface suggests predominantly linear effects of the input parameters, with minimal synergistic interactions or quadratic behavior. This reflects a predictable system, suitable for scaling. Notably, high efficiency values (>90%) were achievable at elevated temperatures and moderate-to-high flow rates, suggesting an optimal operational envelope.

The response trend aligns with current mechanistic understanding of organosolv processes, where elevated temperatures promote the cleavage of linkages that will release soluble lignin fragments to the carbohydrate matrix. Increased thermal energy accelerates both solvolysis and acid-catalyzed cleavage of β-O-4 bonds and potentially lignin-carbohydrate complexes (LCCs), thereby enhancing delignification efficiency.[38]
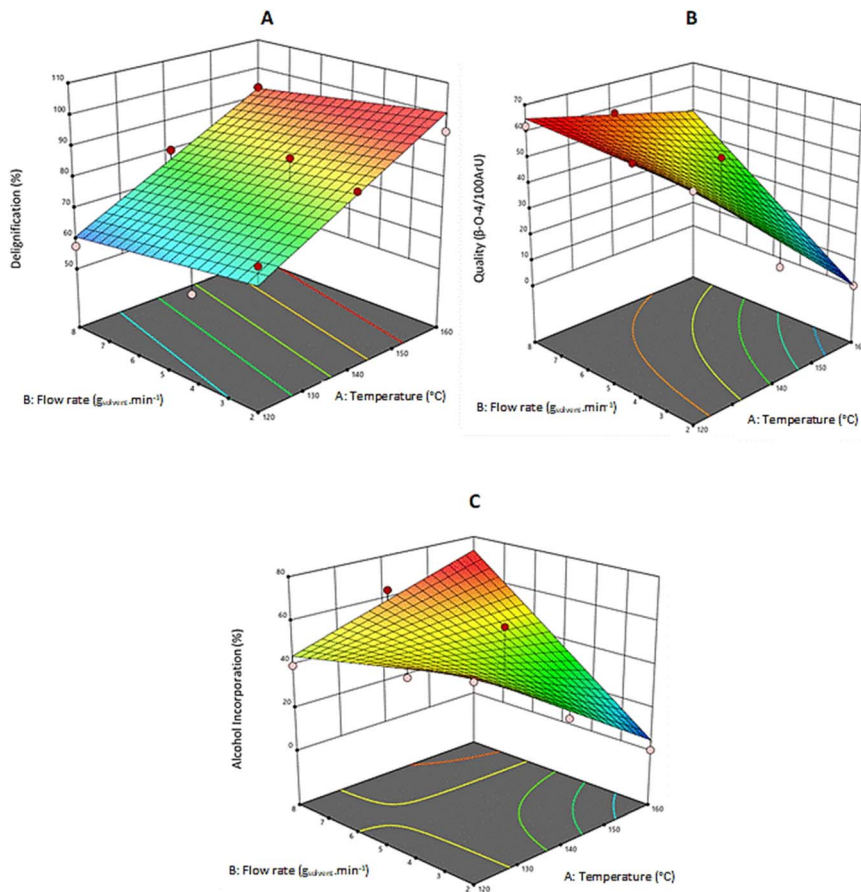
Fig. 8 RSM 3D Models showing the effects of extraction temperature and flow-rate on investigated responses; (A)-delignification efficiency, (B)-lignin quality & (C)-alcohol incorporation.

Table 5 Statistical evaluation of optimization models (a difference of not more than 0.2 between adjusted R^2 and predicted R^2 indicates good model predictability and internal consistency. An adequate precision greater than the threshold of 4.0 suggests a good signal-to-noise ratio, confirming that a model is sufficiently robust for exploration and optimization within the defined design space)

Model	Adjusted R^2	Predicted R^2	Adequate precision
Delignification efficiency model (A)	0.81	0.67	10.2
Lignin quality model (B)	0.85	0.77	10.3
Alcohol incorporation model (C)	0.75	0.31	8.5

The model describing lignin quality (B), based on the conservation of β-O-4 linkages, provides critical insight into the influence of extraction severity on the structural integrity of the recovered lignin.

The response surface model for lignin quality demonstrates a bell-shaped contour, suggesting a delicate balance between conditions used and structural preservation. At low to moderate temperatures (120–140 °C) and intermediate flow rates, the highest β-O-4 linking motif retention (>60%) is observed. However, beyond this window, particularly at higher temperatures (140–160 °C) and low flow rates (2 $g_{solvent}$ min^{-1}), a steep decline in bond preservation occurs. This behavior indicates that while harsher conditions improve delignification, they also promote acidolysis and condensation reactions that degrade the β-O-4 architecture, forming C–C bonded lignin fragments that are less reactive and more recalcitrant.[13,41]

The model's curvature suggests that both parameters interact synergistically to influence bond conservation. Specifically, a high flow rate may mitigate the negative impact of elevated temperatures by reducing residence time and swiftly removing reactive lignin intermediates. This supports recent literature advocating for fast lignin removal to preserve labile bonds, and enhanced yield of functional lignin.[42]

Model C tracks the extent of alcohol incorporation from the extraction solvent (ethanol) into lignin *via* chemical modification of β-O-4 linkages. This phenomenon is indicative of stabilization *via* acetal or ether formation,[43,44] which serves to cap reactive intermediates and prevent condensation. It was noted that the difference between the predicted R^2 and adjusted R^2 was greater than 0.2 and hence makes the model's predictability significantly limited. This difference may be attributed to a large block effect which requires further experimentation to resolve. However, the adequate precision value of the model was 8.5079, which is greater the threshold value of 4 for the signal-to-noise ratio implying that this model can still be used to navigate the design space.

The response surface displays a clear trend of increasing alcohol incorporation with rising temperatures and flow rates. Maximum incorporation (>60%) occurs at high temperatures (160 °C) combined with high flow rates (8.0 $g_{solvent}$ min^{-1}), pointing to conditions that favor both chemical reactivity and efficient extraction. Elevated temperature promotes the activation of lignin's α-hydroxyaryl units, which can readily undergo etherification with alcohols under acidic conditions.[41] Simultaneously, high flow rates reduce the likelihood of secondary degradation or cross-linking by quickly flushing out the modified lignin.

This model underscores a vital consideration in lignin-first biorefining strategies: that alcohol not only functions as a solvent but also participates directly in lignin stabilization. The incorporation of solvent-derived fragments into β-O-4 linkages has been shown to improve solubility, reduce molecular weight distribution, and enhance compatibility with downstream functionalization pathways.[45,46] However, excessive incorporation may also alter the native lignin structure beyond desirable limits, emphasizing the importance of tuning process conditions based on end-use requirements.

The model's shape suggests positive synergy between temperature and flow rate, where both variables must be optimized concurrently to maximize incorporation while preserving functional moieties.

3.4.1 **Optimized extraction model validation.** Using computational modelling, an optimization framework was developed for lignin extraction in the semi-continuous flow-through system. The predictive model simultaneously considered two key response variables, delignification efficiency and lignin quality, with

Table 6 Optimal extraction parameters with predicted response values from the model

Temperature (°C)	Flow rate ($g_{solvent}$ min^{-1})	Predicted delignification (wt%)	Predicted lignin quality (β-O-4 per 100 ArU)
145–151	8	81–87	≥52

equal weighting assigned to both parameters. Table 6 presents the derived optimal extraction conditions along with their predicted performance outcomes.

The optimal extraction conditions, determined computationally, were validated experimentally under the operational parameters of a temperature of 150 °C and a solvent flow rate of 8.0 $g_{solvent}$ min^{-1}, resulting in 82 wt% delignification efficiency and 59.4 β-O-4 linkages per 100ArU, which is well within the computationally predicted range of 81–87 wt% and minimum threshold of ≥52 β-O-4 linkages per 100ArU for the operational parameters employed (8 $g_{solvent}$ min^{-1} flow rate at 150 °C). It must be noted that the optimal flow rate of 8 $g_{solvent}$ min^{-1} predicted by the model is dependent on the reactor's maximum capacity, which is the same and therefore it is possible that higher flow rates may be desirable for higher capacity reactors.

2D HSQC NMR characterization of the lignin obtained from the optimized run revealed 59.4 β-O-4 linkages per 100ArU, surpassing the predicted minimum threshold of ≥52, alongside a high alcohol incorporation rate of 62.8%. Furthermore, the lignin exhibited an S/G ratio of 4.9, while demonstrating moderate S-unit condensation at 14.5%. The observed S_{cond} remains within acceptable limits for downstream valorization and reflects expected behavior under these extraction conditions.[47] Collectively, these structural parameters demonstrate that the optimized conditions successfully balanced the inherent trade-offs between delignification efficiency and lignin quality preservation and outperformed similar methods used for the extraction of lignin, including deep-eutectic-solvent extractions, steam explosion and hydrothermal pretreatment followed by ethanol/water extractions.[48,49] Also worth mentioning is that the results obtained for β-O-4 content conservation for this optimized ethanosolv extraction, 59.4 β-O-4 linkages per 100ArU, comes close to results obtained with butanosolv extractions, 66 β-O-4 per 100ArU, reported in the literature,[23] but the process with ethanol is deemed more suitable due to easier purification and lower cost.

3.4.2 Solvent optimization. The UV-Vis kinetic profile of the optimized run as seen in Fig. 9 suggests that beyond a certain solvent volume, the rate of lignin extraction significantly slows, suggesting an equilibrium where most of the extractable lignin has already been removed. This finding highlights the potential for optimizing solvent usage to minimize waste and reduce costs, further enhancing the potential for industrial application of this system. The optimal solvent cut-off is determined by identifying where the extraction rate derivative falls below 5% of its maximum value.

The derivative in this context represents the rate of change of extracted lignin mass with respect to solvent use, calculated as:

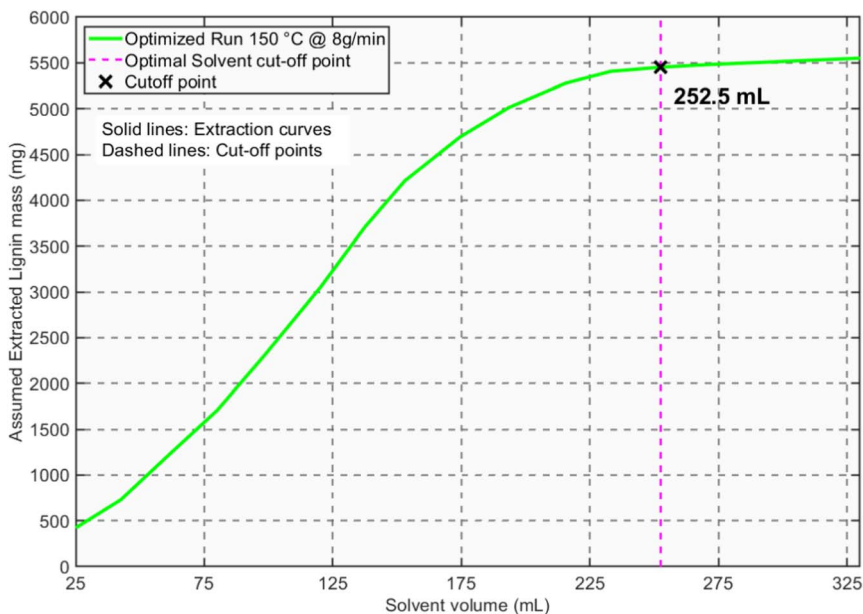$$\frac{\Delta M}{\Delta S_v} = \frac{M(i+1) - M(i)}{S_v(i+1) - S_v(i)}$$

Fig. 9 Plot of accumulated lignin mass *vs.* solvent use with the solvent cut-off point for the optimized run of 150 °C at 8 $g_{solvent}$ min^{-1}.

where M = extracted lignin mass (mg) and S_v = volume of used solvent (mL)

The solvent cut-off point was defined as the time at which the first derivative of the extraction rate dropped below 5% of its maximum observed value (1.90 g mL^{-1}, corresponding to 5% of the peak rate of 37.98 g mL^{-1}). This threshold signifies the onset of diminishing extraction efficiency, where further processing yields minimal improvements in mass transfer. The complete kinetic profile and the identified cut-off point are shown in Fig. 9 (see SI Table S6 for details of the derivative analysis). The solvent cut-off point of 252.5 mL implies a 13.1 $mL_{solvent}$ $g_{biomass}^{-1}$ solvent-to-biomass ratio. Compared to the original solvent-to-biomass ratio for the flow-through extractions, expressed as 18 $mL_{solvent}$ $g_{biomass}^{-1}$, we observe a 4.9 mL reduction in the solvent requirement per gram of biomass. This indicates a recalibration of the total extraction time for the determined optimal flow rate (8 g.min^{-1}) in this study. Based on the volumetric flow rate of 9.4 mL min^{-1} that was recorded from the experimental runs (see Table 4), the optimized extraction would have a new duration calculated as follows:

$$\text{Total extraction time (min)} = \frac{252.5 \text{ mL}}{9.4 \text{ mL min}^{-1}} = 27 \text{ min}$$

This change represents a further decrease from the previous 38-minute period to process a 360 mL solvent volume at a 8 g min^{-1} flow rate to just under 30 minutes and demonstrates the feasibility of process intensification opportunities *via* solvent reduction. When comparing the optimised conditions (8 g min^{-1}, 13.1 mL g^{-1} solvent : biomass, 27 minutes) to the standard extraction protocol used in previous studies[22–24,29] (2 g min^{-1}, 18.0 mL g^{-1} solvent : biomass, 150 minutes), it is clear that the standard setup requires over five times longer and more solvent for the same

biomass loading. This demonstrates the large gains in time and solvent usage that can be achieved through tuning flow and solvent use appropriately. Effective use of solvents can reduce the time and energy required to complete a process, while also reducing the cost and environmental impact of downstream solvent recovery.

Furthermore, the optimal ratio (13.1 $\text{mL}_{\text{solvent}}$ $\text{g}_{\text{biomass}}^{-1}$) represents over 40% less usage of solvent when compared to the solvent : biomass ratio of 22.9 $\text{mL}_{\text{solvent}}$ $\text{g}_{\text{biomass}}^{-1}$ for batch organosolv lignin extractions on a lab scale.[50,51] The results obtained demonstrate that, under optimized laboratory conditions, the flow-through reactor outperforms the batch reactor, and its performance approaches that of pilot-scale Fabiola™ extractions (5 mL g^{-1}) in terms of solvent usage.[52] Although the flow-through reactor requires slightly more solvent, it yields significantly higher lignin quality (the reported process shows between 4 and 10 β-O-4 linkages per 100ArU for ethanol extractions and approximately 35 β-O-4 linkages per 100 ArU for acetone extraction) and substantially reduces operational times (from 2 hours to about 30 min) compared to the batch method.

These results collectively demonstrate that the computationally optimized flow-through extraction process achieves efficient, predictable, and controllable delignification of birch-wood biomass, with performance parameters that remain stable across multiple experimental validations while significantly reducing the total extraction time.

4 Conclusion

This study demonstrates the successful optimization and validation of a flow-through organosolv system for lignin extraction from birch wood. The computational model predicted high lignin extraction efficiency (81–87 wt%) with substantial retention of β-O-4 linkages ($\geq$52 per 100 aromatic units) under optimized conditions (temperature range: 145–151 °C, flow rate 8 $\text{g}_{\text{solvent}}$ min^{-1}). These predictions were validated experimentally, where 82 wt% delignification was achieved at 150 °C and a flow rate of 8 $\text{g}_{\text{solvent}} \cdot \text{min}^{-1}$, closely matching the model's predictions. 2D HSQC NMR revealed 59.4 β-O-4 linkages per 100 aromatic units and 62.8% alcohol incorporation, indicating strong structural integrity, with an S/G ratio of 4.9 and limited condensation. These values surpass those realized from similar works where only 48 wt% delignification and a β-O-4 linkage conservation of 12 per 100 ArU were seen in birch-wood lignin extractions. Under optimized conditions, the process also demonstrated a solvent-to-biomass ratio of 13.1 $\text{mL}_{\text{solvent}}$ $\text{g}_{\text{biomass}}^{-1}$, resulting in a 40% reduction in solvent usage when compared to some laboratory-scale batch reactors, also showing a significant decrease in operational time from two hours to approximately 30 minutes. Mechanistically, the model and experiments showed that temperature primarily governs extraction efficiency, while higher flow rates effectively minimize thermal degradation of β-O-4 linkages, enabling optimal performance at 150 °C. The robust agreement between computational predictions and experimental results demonstrates the reliability of the model and the potential of this optimized approach for efficient, high-quality lignin extraction.

Conflicts of interest

The authors declare that there are no known conflicts of interest involved in this work.

Data availability

All data is available in the manuscript and accompanying SI. See DOI: https://doi.org/10.1039/d5fd00104h.

References

1 Natural Resources Canada, Forest Products from Birch Trees, *Natural Resources Canada*, 2017.

2 G. Baumann, R. Brandner, U. Müller, C. Kumpenza, A. Stadlmann and F. Feist, Temperature-related properties of solid birch wood under quasi-static and dynamic bending, *Materials*, 2020, **13**(23), 1–23, DOI: 10.3390/ma13235518.

3 D. Godina, G. Sosins, A. Paze, J. Rizikovs, R. Makars and A. Treu, Evaluating the Potential of Birch Bark Suberinic Acids for Solid Wood Impregnation, *J. Renewable Mater.*, 2025, **13**(1), 147–161, DOI: 10.32604/jrm.2024.056822.

4 Z. Wang and P. J. Deuss, The isolation of lignin with native-like structure, *Biotechnol. Adv.*, 2023, **68**, 108230, DOI: 10.1016/j.biotechadv.2023.108230.

5 M. Balakshin, E. Capanema, R. Santos, H. M. Chang and H. Jameel, Structural analysis of hardwood native lignins by quantitative 13C NMR spectroscopy, *Holzforschung*, 2016, **70**, 95–108, DOI: 10.1515/hf-2014-0328.

6 J. Reiter, H. Strittmatter, L. O. Wiemann, D. Schieder and V. Sieber, Enzymatic cleavage of lignin β-O-4 aryl ether bonds via net internal hydrogen transfer, *Green Chem.*, 2013, **15**(5), 1373–1381, DOI: 10.1039/C3GC40295A.

7 Z. H. Liu, N. Hao, Y. Y. Wang, *et al.*, Transforming biorefinery designs with 'Plug-In Processes of Lignin' to enable economic waste valorization, *Nat. Commun.*, 2021, **12**(1), 3912, DOI: 10.1038/s41467-021-23920-4.

8 F. Brienza, D. Cannella, D. Montesdeoca, I. Cybulska and D. P. Debecker, A guide to lignin valorization in biorefineries: traditional, recent, and forthcoming approaches to convert raw lignocellulose into valuable materials and chemicals, *RSC Sustainability*, 2024, **2**(1), 37–90, DOI: 10.1039/D3SU00140G.

9 T. I. Korányi, B. Fridrich, A. Pineda and K. Barta, Development of 'Lignin-First' Approaches for the Valorization of Lignocellulosic Biomass, *Molecules*, 2020, **25**(12), 2815, DOI: 10.3390/molecules25122815.

10 D. Raikwar, S. Majumdar and D. Shee, Thermocatalytic depolymerization of kraft lignin to guaiacols using HZSM-5 in alkaline water–THF co-solvent: a realistic approach, *Green Chem.*, 2019, **21**(14), 3864–3881, DOI: 10.1039/C9GC00593E.

11 S. Agarwal, R. K. Chowdari, I. Hita and H. J. Heeres, Experimental Studies on the Hydrotreatment of Kraft Lignin to Aromatics and Alkylphenolics Using Economically Viable Fe-Based Catalysts, *ACS Sustain. Chem. Eng.*, 2017, **5**(3), 2668–2678, DOI: **10.1021/acssuschemeng.6b03012**.

12 A. Rahimi, A. Ulbrich, J. J. Coon and S. S. Stahl, Formic-acid-induced depolymerization of oxidized lignin to aromatics, *Nature*, 2014, **515**(7526), 249–252, DOI: **10.1038/nature13867**.

13 L. Shuai, M. Talebi Amiri, Y. Questell-Santiago, *et al.*, Formaldehyde stabilization facilitates lignin monomer production during biomass depolymerization, *Science*, 1979, **354**, 329–333, DOI: **10.1126/science.aaf7810**.

14 P. J. Deuss, C. S. Lancefield, A. Narani, J. G. de Vries, N. J. Westwood and K. Barta, Phenolic acetals from lignins of varying compositions via iron(iii) triflate catalysed depolymerisation, *Green Chem.*, 2017, **19**(12), 2774–2782, DOI: **10.1039/C7GC00195A**.

15 H. Zhou, J. Y. Xu, Y. Fu, *et al.*, Rapid flow-through fractionation of biomass to preserve labile aryl ether bonds in native lignin, *Green Chem.*, 2019, **21**(17), 4625–4632, DOI: **10.1039/C9GC02315A**.

16 J. H. Jang, A. R. C. Morais, M. Browning, *et al.*, Feedstock-agnostic reductive catalytic fractionation in alcohol and alcohol–water mixtures, *Green Chem.*, 2023, **25**(9), 3660–3670, DOI: **10.1039/D2GC04464A**.

17 Y. Zhu, Y. Liao, L. Lu, W. Lv, J. Liu, X. Song, J. Wu, L. Li, C. Wang, L. Ma and B. F. Sels, *ACS Catal.*, 2023, **13**(12), 7929–7941, DOI: **10.1021/acscatal.3c01309**.

18 S. Zheng, S. Sun, L. P. Manker and J. S. Luterbacher, Aldehyde-Stabilization Strategies for Building Biobased Consumer Products around Intact lignocellulosic Structures, *Acc. Chem. Res.*, 2025, **58**(6), 877–892, DOI: **10.1021/acs.accounts.4c00819**.

19 T. Renders, G. Van den Bossche, T. Vangeel, K. Van Aelst and B. Sels, Reductive catalytic fractionation: state of the art of the lignin-first biorefinery, *Curr. Opin. Biotechnol.*, 2019, **56**, 193–201, DOI: **10.1016/j.copbio.2018.12.005**.

20 P. J. Deuss, M. Scott, F. Tran, N. J. Westwood, J. G. de Vries and K. Barta, Aromatic Monomers by in Situ Conversion of Reactive Intermediates in the Acid-Catalyzed Depolymerization of Lignin, *J. Am. Chem. Soc.*, 2015, **137**(23), 7456–7467, DOI: **10.1021/jacs.5b03693**.

21 C. W. Lahive, P. J. Deuss, C. S. Lancefield, *et al.*, Advanced Model Compounds for Understanding Acid-Catalyzed Lignin Depolymerization: Identification of Renewable Aromatics and a Lignin-Derived Solvent, *J. Am. Chem. Soc.*, 2016, **138**(28), 8900–8911, DOI: **10.1021/jacs.6b04144**.

22 D. Zijlstra, de K. J. Analbers, E. Wilbers and P. Deuss, Efficient Mild Organosolv Lignin Extraction in a Flow-Through Setup Yielding Lignin with High β-O-4 Content, *Polymers*, 2019, **11**, 1913, DOI: **10.3390/polym11121913**.

23 D. S. Zijlstra, J. de Korte, E. P. C. de Vries, *et al.*, Highly Efficient Semi-Continuous Extraction and In-Line Purification of High β-O-4 Butanosolv Lignin, *Front. Chem.*, 2021, **9**, 655983, DOI: **10.3389/fchem.2021.655983**.

24 D. S. Zijlstra, A. de Santi, B. Oldenburger, J. de Vries, K. Barta and P. J. Deuss, Extraction of Lignin with High β-O-4 Content by Mild Ethanol Extraction and Its Effect on the Depolymerization Yield, *J. Visualized Exp.*, 2019, **143**, e58575, DOI: **10.3791/58575**.

25 S. Bertran-Llorens, F. Perondi, A. L. Slama de Freitas, J. Chen, G. van Erven and P. J. Deuss, Supercritical CO2 as effective wheat straw pretreatment for

subsequent mild fractionation strategies, *Chem. Eng. J.*, 2024, **497**, 154491, DOI: **10.1016/j.cej.2024.154491**.

26 A. Kramarenko Logvynenko. Kinetic study of birch wood and walnut shells organosolv delignification in a continuous flow reactor, Poster session presented at 21st Netherlands' Catalysis and Chemistry Conference, 2020.

27 P. Jusner, B. Sridharan, B. Daelemans, *et al.*, Assessing the potential for upscaling the continuous production of lignin oils through reductive catalytic depolymerization, *Chem. Eng. J.*, 2024, **499**, 156474, DOI: **10.1016/j.cej.2024.156474**.

28 A. W. Bartling, M. L. Stone, R. J. Hanes, *et al.*, Techno-economic analysis and life cycle assessment of a biorefinery utilizing reductive catalytic fractionation, *Energy Environ. Sci.*, 2021, **14**(8), 4147–4168, DOI: **10.1039/D1EE01642C**.

29 D. S. Zijlstra, C. W. Lahive, C. A. Analbers, *et al.*, Mild Organosolv Lignin Extraction with Alcohols: The Importance of Benzylic Alkoxylation, *ACS Sustain. Chem. Eng.*, 2020, **8**(13), 5119–5131, DOI: **10.1021/acssuschemeng.9b07222**.

30 A. Sluiter, B. Hames and R. Ruiz, *et al.*, *Determination of Structural Carbohydrates and Lignin in Biomass: Laboratory Analytical Procedure (LAP) (Revised July 2011)*, 2008, **http://www.nrel.gov/biomass/analytical_procedures.html**.

31 J. Xu, Z. Shao, Y. Li, L. Dai, Z. Wang and S. Chuanling, A flow-through reactor for fast fractionation and production of structure-preserved lignin, *Ind. Crops Prod.*, 2021, **164**, 113350, DOI: **10.1016/j.indcrop.2021.113350**.

32 C. Liu and C. E. Wyman, The effect of flow rate of very dilute sulfuric acid on xylan, lignin, and total mass removal from corn stover, *Ind. Eng. Chem. Res.*, 2004, **43**(11), 2781–2788, DOI: **10.1021/ie030754x**.

33 S. Machmudah, K. H. Wahyudiono, M. Sasaki and M. Goto, Hot compressed water extraction of lignin by using a flow-through reactor, *Eng. J.*, 2015, **19**(4), 25–44, DOI: **10.4186/ej.2015.19.4.25**.

34 A. Skulcova, V. Majova, M. Kohutova, M. Grosik, J. Sima and M. Jablonsky, UV/Vis Spectrometry as a Quantification Tool for Lignin Solubilized in Deep Eutectic Solvents, *BioRes.*, 2017, **12**, 6713–6722.

35 P. Schulze, M. Leschinsky, A. Seidel-Morgenstern and H. Lorenz, Continuous Separation of Lignin from Organosolv Pulping Liquors: Combined Lignin Particle Formation and Solvent Recovery, *Ind. Eng. Chem. Res.*, 2019, **58**(9), 3797–3810, DOI: **10.1021/acs.iecr.8b04736**.

36 C. Crestini, F. Melone, M. Sette and R. Saladino, Milled Wood Lignin: A Linear Oligomer, *Biomacromolecules*, 2011, **12**(11), 3928–3935, DOI: **10.1021/bm200948r**.

37 W. Boerjan, J. Ralph and M. Baucher, Lignin Biosynthesis, *Annu. Rev. Plant Biol.*, 2003, **54**(1), 519–546, DOI: **10.1146/annurev.arplant.54.031902.134938**.

38 R. Rinaldi, R. Jastrzebski, M. T. Clough, *et al.*, Paving the Way for Lignin Valorisation: Recent Advances in Bioengineering, Biorefining and Catalysis, *Angew. Chem., Int. Ed.*, 2016, **55**(29), 8164–8215, DOI: **10.1002/anie.201510351**.

39 Z. Wang, Z. Zhang, H. Wang and P. J. Deuss, Tuning lignin properties by mild ionic-liquid-mediated selective alcohol incorporation, *Chem Catal.*, 2022, **2**(6), 1407–1427, DOI: **10.1016/j.checat.2022.04.005**.

40 C. S. Lancefield, I. Panovic, P. J. Deuss, K. Barta and N. J. Westwood, Pretreatment of lignocellulosic feedstocks using biorenewable alcohols: towards

complete biomass valorisation, *Green Chem.*, 2017, **19**, 202–214, DOI: **10.1039/ C6GC02739C**.

41 M. V. Galkin and J. S. M. Samec, Lignin Valorization through Catalytic Lignocellulose Fractionation: A Fundamental Platform for the Future Biorefinery, *ChemSusChem*, 2016, **9**(13), 1544–1558, DOI: **10.1002/ cssc.201600237**.

42 X. Luo, Y. Li, N. K. Gupta, B. Sels, J. Ralph and L. Shuai, Protection Strategies Enable Selective Conversion of Biomass, *Angew. Chem.*, 2020, **132**(29), 11800– 11812, DOI: **10.1002/ange.201914703**.

43 A. De Santi, S. Monti, G. Barcaro, Z. Zhang, K. Barta and P. J. Deuss, New Mechanistic Insights into the Lignin β-O-4 Linkage Acidolysis with Ethylene Glycol Stabilization Aided by Multilevel Computational Chemistry, *ACS Sustain. Chem. Eng.*, 2021, **9**(5), 2388–2399, DOI: **10.1021/ acssuschemeng.0c08901**.

44 Z. Zhang, C. W. Lahive, J. G. M. Winkelman, K. Barta and P. J. Deuss, Chemicals from lignin by diol-stabilized acidolysis: reaction pathways and kinetics, *Green Chem.*, 2022, **24**(8), 3193–3207, DOI: **10.1039/D2GC00069E**.

45 T. Renders, S. den Bosch, S. F. Koelewijn, W. Schutyser and B. F. Sels, Lignin- first biomass fractionation: the advent of active stabilisation strategies, *Energy Environ. Sci.*, 2017, **10**(7), 1551–1557, DOI: **10.1039/C7EE01298E**.

46 M. M. Abu-Omar, K. Barta, G. T. Beckham, *et al.*, Guidelines for performing lignin-first biorefining, *Energy Environ. Sci.*, 2021, **14**(1), 262–292, DOI: **10.1039/d0ee02870c**.

47 C. Lancefield, O. Ojo, F. Tran and N. Westwood, Isolation of Functionalized Phenolic Monomers through Selective Oxidation and CO Bond Cleavage of the β-O-4 Linkages in Lignin, *Angew. Chem., Int. Ed.*, 2015, **54**, 258–262, DOI: **10.1002/anie.201409408**.

48 L. da Costa Sousa, M. Foston, V. Bokade, *et al.*, Isolation and characterization of new lignin streams derived from extractive-ammonia (EA) pretreatment, *Green Chem.*, 2016, **18**(15), 4205–4215, DOI: **10.1039/C6GC00298F**.

49 J. Li, G. Henriksson and G. Gellerstedt, Lignin depolymerization/ repolymerization and its critical role for delignification of aspen wood by steam explosion, *Bioresour. Technol.*, 2007, **98**(16), 3061–3068, DOI: **10.1016/ j.biortech.2006.10.018**.

50 L. Y. Liu, S. C. Patankar, R. P. Chandra, N. Sathitsuksanoh, J. N. Saddler and S. Renneckar, Valorization of Bark Using Ethanol–Water Organosolv Treatment: Isolation and Characterization ofCrude Lignin, *ACS Sustain. Chem. Eng.*, 2020, **8**(12), 4745–4754, DOI: **10.1021/acssuschemeng.9b06692**.

51 Y. Mao, I. Tarhanli, G. Owen, C. S. Lee, E. Senses and E. Binner, Comparisons of alkali, organosolv and deep eutectic solvent pre-treatments on the physiochemical changes and lignin recovery of oak and pine wood, *Ind. Crops Prod.*, 2025, **226**, 120614, DOI: **10.1016/j.indcrop.2025.120614**.

52 A. Smit and W. Huijgen, Effective fractionation of lignocellulose in herbaceous biomass and hardwood using a mild acetone organosolv process, *Green Chem.*, 2017, **19**(22), 5505–5514, DOI: **10.1039/C7GC02379K**.